Characterization of Metal Nanoparticles Aqueous Solution by a Thermoelastic Optical Indicator Microscope

G. A. Ohanyan[a], N. G. Margaryan[a], M. T. Manvelyan[a], L. A. Odabashyan[a], B. J. Minasyan[a], A. J. Movsisyan[a], R. Zh. Khachatryan[b], and A. Zh. Babajanyan[a], *

[a] Yerevan State University, Yerevan, Armenia
[b] Institute of Radiophysics and Electronics, NAS of Armenia, Ashtarak, Armenia
*e-mail: barsen@ysu.am

Abstract—The aqueous solution with different metal nanoparticles (NPs) characterized by a thermoelastic optical indicator microscope (TEOIM) in microwave range (8−12 GHz). The near-field interaction between radiated microwaves and aqueous solution with Ag, Zn, and Fe NPs prepared by a laser ablation process is sensitive to NPs concentration and structural characteristics in the solution at resonant frequency. The examined metal NPs maximum concentrations were 50 μg/L. The measured minimum detectable normalized signal was 0.0547, 0.0381, 0.0333 $(\mu g/L)^{-1}$ and the measured minimum detectable concentration was about 1, 0.7, 0.6 μg/L for the Ag, Zn, Fe, respectively. Such sensitive response of measurement system can be explained not only by the electromagnetic specification variation (complex dielectric permittivity, conductivity etc.) of solution due to change of metal NPs concentration, but also by the additional structural changes in water clusters due to the NPs ablation process. In addition, TEOIM characterization method allows to visualize the electromagnetic field distribution around solution with high spatial resolution in term to investigate the dielectric liquid environment with different type and concentrations of high-conductive NPs.

1. INTRODUCTION

Nowadays, nanoparticles (NPs) have become an integral part of practical industrial systems. NPs are represented the system of atoms in the size range less than 100 nanometers. NPs are categorized by their physical parameters, such as electrical and chemical properties, shapes, morphology. Depended on their properties the application of the NPs is variety. In material industry they can be useful for manufacturing scratchproof eyeglasses, crack-resistant paints, anti-graffiti coatings for walls, transparent sunscreens, stain-repellent fabrics, and self-cleaning windows. In agricultural sphere it can be useful for plant health management and soil improvement. The NPs are also applicable in modern medicine. By using NPs, it can provide more accuracy in traditional biological imaging of cells and tissues using fluorescence microscopy as well as in modern magnetic resonance imaging of various regions of the body [1−4].

Our study particularly related to NPs of Zinc (Zn), Iron (Fe) and Silver (Ag). As above mentioned, metal NPs have also various applications in different types of spheres. All this three NPs has great impact of water, wastewater treatment and can affect to improve treatment efficiency. In some experimental results suggest that Zinc oxide (ZnO) NPs due to their antibacterial properties can potentially be an antibacterial reagent to treat wastewater [5]. The NPs of Iron has a like small size, high surface area, and magnetic property and due to this feature Iron oxide (FeO) NPs are used for removing contamination (heavy metals) in water [6]. Like FeO NPs, Ag NPs also using for removing heavy metals from water. Instead of that Ag NPs have important role in aqueous solutions. In view of health care, the right amount of Ag NPs in drinking water is important. Due to its biologically active properties Ag NPs in distilled water can be remedy of treatment in medicine and also can be applicable in pharmacology [7, 8]. Above mentioned Ze, Fe, and Ag NPs has common applications related to aqueous solution and hence there is important task to determine their concentration in aqueous solutions.

In our previous studies we determined the concentration of Ag and Fe NPs in aqueous solution by microwave sensing method with using microstrip resonators [9, 10]. The experimental results were accu-
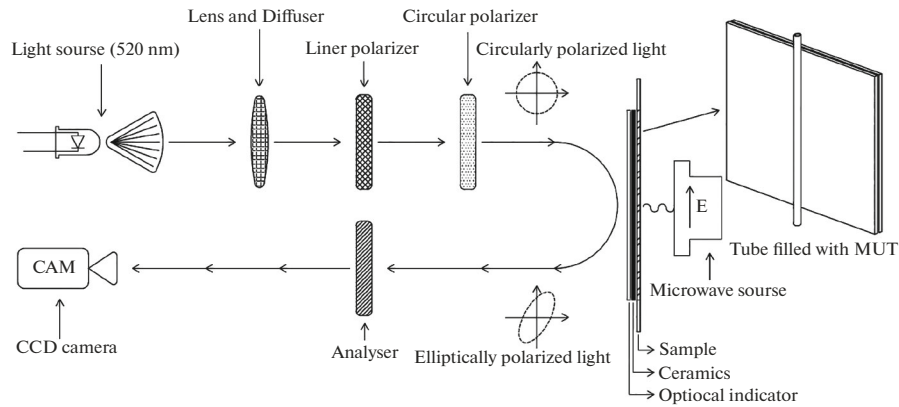
Fig. 1. Schematic diagram of a TEOIM system: optical subsystem (left part) and microwave subsystem (right part).

rate and promising for future development of biomedical non-invasive sensors. In this study we investigate the change of concentration of Ag, Zn, and Fe NPs in aqueous solution by using thermoelastic optical indicator microscope (TEOM) [11, 12]. Compare to previous method this technique is able to provide visual demonstration of radiated microwave spatial distribution depend on NPs concertation and type. The experiments were carried out with microwaves in frequency range of 8−12 GHz (X-band). The experimental results suggests that TEOM technique can serve as a biophysical sensor and is convenient tool for providing visual demonstration of the change of concentration of NPs in liquid environment without scanning.

2. MATERIALS AND METHODS

Ag, Zn, and Fe NPs aqueous solutions were investigated by TEOIM. The schematic diagram of TEOIM system is shown in Fig. 1. TEOIM consists of two subsystems. First subsystem is optical part where was measured the polarization change due to microwave−sample interaction and the second subsystem is microwave part where optical indicator with material under test (MUT) is irradiated from microwave source and acts as a heat source. As microwave source used microwave generator−microwave signal amplifier−coaxial to waveguide adapter system.

A microwave signal was generated by R&S SMA100B and passed to Mini-Circuits ZVE-3W-183+ amplifier after which the amplified signal was transferred to Pasternak WR-90 coaxial to waveguide adapters input. During the experiment microwave source generated the signal in 8−12 GHz frequency range. Microwave radiation is directed to OI with MUT. Between the OI and microwave source was placed the MUT which is the silicon tube with 0.8 mm inner diameter filled with NPs aqueous solution. Due to microwaves interaction with MUT the thermal stresses in OI is occur, which is detected by optical subsystem of TEOIM. In optical subsystem the radiated 520 nm green light passing through the linear polarizer and circular polarizer lenses is becoming circularly polarized. Circular polarized light reflecting from OI is changing its polarization from circular to elliptical in a result of thermoelastic effect. The reflected elliptically polarized light passing through the analyzer was recorded by CCD camera. The CCD camera is measuring the polarization change in each point (pixel) based on the reflected light intensity change, for two positions of analyzer (0° and 45°). OI is one of the most important components of the system and is made of glass which is coated by a indium-thin oxide (ITO) with 150 nm thickness that absorbs the in-plane magnetic component of the incident microwave field and generates heat distribution on OI.

The metal NPs aqueous solutions were prepared by infrared (1060 nm) laser ablation process [9]. The experimental results for metal NPs aqueous solution compared with results of de-ionized (DI) water.

3. RESULTS AND DISCUSSION

The distribution of the magnetic field component of microwaves (Fig. 2a) radiated from the WR-90 open-ended waveguide has a Gaussian form and further used as a microwave source. The visualized magnetic near-field (MNF) distribution at 11 GHz at a distance of 1 mm from MUT is shown in Figs. 2b−2e. For MUT filled with DI-water the MNF distribution has form of tube with width exiting the inner diam-
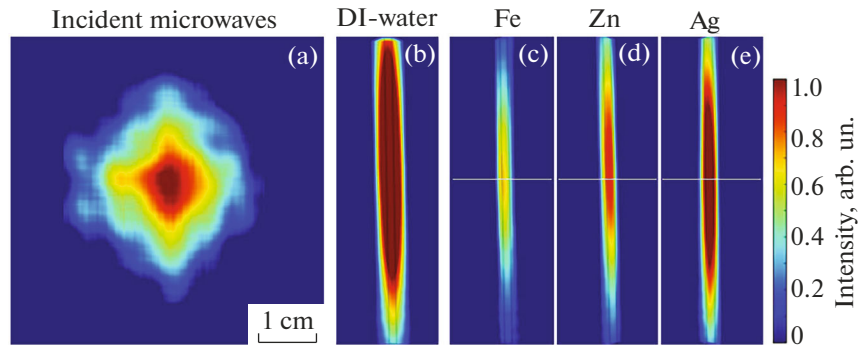
Fig. 2. (a) Normalized magnetic field distribution for incident microwaves, and MNF distributions around MUT filled with (b) DI-water, (c) Fe, (d) Zn, (e) Ag NPs at 11 GHz. The black rectangles represent the contours of tube inner space.
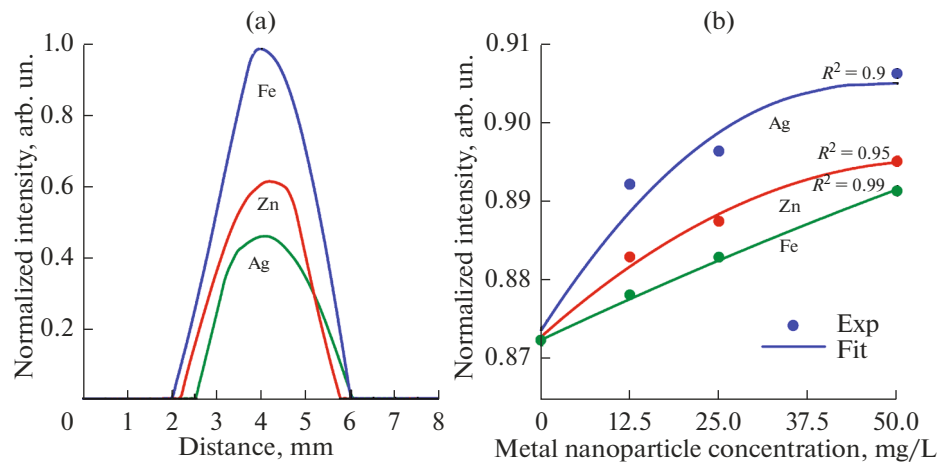

Fig. 3. (a) Cross-sectional profiles of normalized MNF images obtained from Figs. 2c−2e along white solid lines. (b) The average intensity calculated from normalized MNF image vs. NPs concentration for different metals at the operating frequency of 11 GHz.

eter of tube (or diameter of solution) as one can see in Fig. 2b. The MNF distributions for MUT with aqueous solution with metal NPs are presented in Fig. 2c for Fe, 2d for Zn, and 2e for Ag. Note that in contrast of DI-water image, the MNF distributions for MUTs with different metal NPs here are presented as subtraction images of NPs and DI-water with different scales of color-bar (normalized by a maximum of intensity on each scale) for Figs. 2a−2b and Figs. 2c−2e. Cross-sectional profiles along white solid lines of the normalized MNF for different MUT are shown in Fig. 3a. As metal conductivity increased (Fe: 9.9 MS/m, Zn: 16.8 MS/m, Ag: 61.4 MS/m), the intensity of the MNF increased (about 2.1 times for Fe to Ag). This behavior is well observed both for distribution images and for cross-sectional profiles.

As we can see from Fig. 3b the average intensity of MNF had shown increasing behavior when the concentration of the NPs in solution was increased but with different rate for each metal: 0.0333, 0.0381, 0.0547 $(\mu g/L)^{-1}$, for Fe, Zn, Ag, respectively. A clear correlation between averaged intensity of MNF (and distribution of MNF) growth rate and metal conductivity is well observed. The measured minimum detectable concentration based on the coefficient of determination (R^2) was about 0.6, 0.7, and 1.0 $\mu g/L$ for the Fe, Zn, and Ag, respectively.

Figure 4 plots averaged MNF intensity as a function of the incident frequency in the range of 10−12 GHz. One sees that the averaged MNF intensity has a maximum at 11 GHz. However, a resonant frequency shift due to the changes in the conductivity of the metal of NPS is not observed. The reason of high excitation intensity at 11 GHz is an experimental configuration limited by the optimal operating frequency range of the WR-90 waveguide (8.2−12.4 GHz), OI, and characteristics of the coupling between MUT and microwave radiation. Thus, 11 GHz was chosen as an optimal frequency for the visualization and monitoring of the concentration of metal NPs.
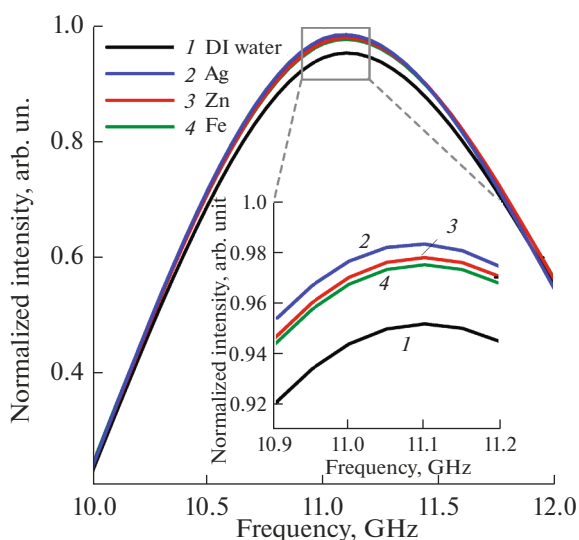
Fig. 4. Frequency responses of the averaged MNF for MUT filled with DI-water and with Fe, Zn, Ag NPs aqueous solution with 50 µg/L concentration for all metals. Inset shows the enlarged region of resonant maximum.

As mentioned in our previous works [9, 10], the measured intensity signal difference (Di-water vs. 50 µg/L concentration of Fe or Ag NPs nanoparticles aqueous solution) do not caused only NPs concentration change which is in order of 10^{-8}. Therefore, the change in measured signal cannot cause by changes in complex permittivity of solution. Thus, we assume that the high microwave response of MUT is caused by structural changes in water due to presence of metal NPs. NPs as the colloidal particles form the bigger structural zones in water in sizes exceed their own sizes and increase the absorbing ability of the system. In addition, the presence of metallic NPs in the liquid initiates eddy currents around the NPs, which causes additional changes in OI. Therefore, the microwave response is much greater than that caused by change in complex permittivity only. In summary, the reason of measurable shift in visualized signal is the specifically textured structure of metal NPs/water system. However, future investigations are needed to discover the clear mechanism of these structural changes.

4. CONCLUSION

The TEOIM system was applied to monitoring metal NPs concentration in aqueous solution by non-invasive method. The MNF distribution for MUT with Fe, Zn, and Ag NPs aqueous solution visualized at 11 GHz. The rates of linear approximated relationship between averaged MNF intensity and NPs concentrations correlated with conductivity of metals of the NPs: both higher conductivity and higher concentration provide bigger signal change. We assume that the measurable change in visualization intensity is caused by structural changes in water formed by metal NPs. The TEOIM method demonstrated ability for monitoring of the high conducting NPs concentration in dielectric liquid environment for chemical and biophysical sensing applications.

FUNDING

CONFLICT OF INTEREST

The authors declare no conflict of interest.

REFERENCES

1. Khan, I., Saeed, Kh., and Khan, I., *Arabian J. Chem.*, 2019, vol. 12, p. 908.
2. Salata, O.V., *J. Nanobiotechnol.*, 2004, vol. 2, p. 3.

3. Papadaki, D., Kiriakidis, G., and Tsoutsos, Th., *Fundamentals of Nanoparticles*, Ch. 11, Elsevier, 2018, pp. 343−370.

4. Mohajerani, A., Burnett, L., Smith, J. V., Kurmus, H., Milas, J., Arulrajah, A., Horpibulsuk S., and Abdul Kadir, A., *Materials*, 2019, vol. 12, p. 3052.

5. Elmi, F., Alinezhad, H., Moulana, Z., Salehian, F., Mohseni S., Fariba Asgharpour, T., Fallah, H., and Mitra Elmi, M., *Water Sci. Technol.*, 2004, vol. 70, p. 763.

6. Yang, J., Hou, B., Wang, J., Tian, Jingtao Bi, B., Wang, N., Li, X., and Huang, X., *Nanomaterials*, 2019, vol. 9, p. 424.

7. Xu, L., Wang, Y.-Y., Huang, J., Chen, Ch.-Y., Wang, Zh.-X., Xie, H., *Theranostics*, 2020, vol. 10, p. 8996.

8. Singh, M., Singh, Sh., Prasada, S., Gambhir, I. S., *Digest J. Nanomater. Biostructur.*, 2008, vol. 3, p. 115.

9. Odabashyan, L., Margaryan, N., Ohanyan, G., Manvelyana, M., Hambaryana, D., Abrahamyana, T., Khachatryanb, R., and Babajanyana, A., *J. Contemp. Phys.*, 2020, vol. 55 p. 171.

10. Abrahamyan, T., Khachatryan, R., Hambaryan, D., Hovhannisyan, B., Minasyan, B., Odabashyan, L., and Babajanyan, A., *J. Contemp. Phys.*, 2019, vol. 54, p. 196.

11. Lee, H., Arakelyan, Sh., Friedman, B., and Lee, K., *Sci. Rep.*, 2016, vol. 6, p. 39696.

12. Baghdasaryan, Zh., Babajanyan, A., Odabashyan, L., Lee, J.-H., Friedman, B., and Lee, K., *Sci. Rep.*, 2021, vol. 11, p. 2589.

Translated by A. Babajanyan